Two Approaches to Structural Damage Identification: Model Updating vs. Soft Computing

(Revised manuscript, 13 Apr 2005)

Przemysław Kołakowski[♣], Luis E. Mujica[♠], Josep Vehí[♠]
[♣]*SMART-TECH Centre*
Institute of Fundamental Technological Research
Polish Academy of Sciences
Swietokrzyska 21, 00-049 Warsaw, Poland
e-mail: pkolak@ippt.gov.pl
[♠]*Modal Intervals and Control Engineering Lab*
Department of Electronics, Informatics and Automatics
University of Girona, Campus Montilivi
Edifici P-IV, E-17071 Girona, Spain
e-mails: lemujica@eia.udg.es, vehi@eia.udg.es

Key words:

Damage identification, inverse problem, model updating, soft computing, software tools

Abstract

This paper presents two approaches for structural damage identification, each based on a different philosophy. The Virtual Distortion Method is a model-updating method of damage assessment, utilizing gradient-based optimization techniques to solve the resulting inverse dynamic problem in the time domain. Case-Based Reasoning is a soft-computing method utilizing wavelet transformation for signal processing and neural networks for training a base of damage cases to use for retrieving a similar relevant case. Advantages and drawbacks of each approach are discussed. Successful calibration of a numerical model from experiments has been shown as a *sin equa non* for the VDM approach. A numerical example of a beam is presented including a demonstration of the complexity of the inverse problem. Qualitative and quantitative comparisons between the two approaches are made.

1 Introduction

Methods for identifying structural damage can be roughly split into high- and low-frequency-based excitation methods. High-frequency-based methods, for example ultrasonic testing [1], acoustic emission [2], Lamb wave inspection [3], [4], are focused on precise identification of a small defect in a narrow inspection zone. A comprehensive review of high-frequency-based methods is given in [5]. In contrast, low-frequency-based methods (see Section 2.1) use vibration-sensitive parameters to identify significant damage in a relatively broad inspection zone. As examples, high-frequency-based methods are used in aerospace for crack identification in a wing, whilst low-frequency-based methods are used in civil engineering for examining stiffness degradation of a bridge.

The two methods presented in this paper are developed for low-frequency application. The 5FP project PiezoDiagnostics (PD) concentrated on two major goals and provided the incentive. The first goal was to check the ability of piezo-devices for inducing (actuators) and collecting (sensors) the low frequency (below 1 kHz) structural vibration response. The second goal was to develop software tools for performing damage identification by analysing perturbations observed in the response due to stiffness-impairing damage (e.g., corrosion). Applications to engineering infrastructure for transport and storage of fluid media (e.g., pipelines, oil tanks) were considered. The outcome of the software part of the project is the subject of this paper.

Two software packages were developed using two independent approaches. The first approach, Virtual Distortion Method (VDM) developed by the SMART-TECH Centre (STC), belongs to the class of model-updating methods. It uses gradient-based optimization techniques in damage-identification algorithms. The second approach, Case-Based Reasoning (CBR) developed by the Modal Intervals and Control Engineering Laboratory (MICE Lab), belongs to the class of soft-computing methods. It uses wavelet transformation for signal processing and neural networks to match a new damage case with the most relevant previously stored case using similarity criteria.

Sections 2 and 3 overview VDM and CBR, respectively. References to existing SHM methods have been given. Section 4 is devoted to numerical model calibration. Section 5 describes a numerical example of a simple beam using both methods. Demonstration of the complexity of the inverse problem has been included. Section 6 contains conclusions and remarks on the two approaches.

2 VDM-based approach

2.1 VDM vs. model-updating methods

This section describes the use of VDM for damage assessment. A finite element model is built and modified to determine parameters identifying the location of damage and to quantify its intensity.

Most low-frequency vibration-based methods for damage identification require a finite element model. Several damage-sensitive parameters of the model are selected for diagnosing structural health. The damage identification procedure consists of updating the model parameters to best match an experimental response of a damaged structure. A resulting inverse problem has to be solved. Natural frequencies and mode shapes are often used for assessing damage [6], [7]. Anti-resonance frequencies can improve the accuracy of damage predictions [8].

Modal curvature was identified as a damage-sensitive parameter [9]. The SHM algorithms also contained modal strain energy [10] [11] and modal kinetic energy [12] as parameters. Efficiency improvement from model reduction is an important issue in model updating [13]. Bridges are real structures for which validations of SHM methods have been frequently performed [14], [15], [16]. An interesting alternative to inverse methods in damage assessment is the Direct Stiffness Calculation Method proposed in [17].

VDM has been developed over many years by STC. It has been classified as a fast reanalysis method in [18]. It is very efficient where an original response of a structure is known. Modifications to its behaviour can be introduced without repeating the whole analysis. Various problems of structural mechanics can be solved using VDM, for example progressive collapse, structural remodelling, damage identification, vibration control, and adaptive structure design. Application of VDM as a tool for system (water networks) modelling and diagnostics has been recently studied in [19].

Modelling local structural modifications is achieved by introducing a corresponding *virtual distortion* ε^o, which is an initial strain, imposed locally in an element of a discrete (truss) or discretized (beam) structure. The VDM reanalysis can be performed very quickly (with no iterations because of the known initial strain) using the so-called *influence matrix* D, which is always created as a basis for all computations. The influence matrix defines all local–global inter-relations for a structure, including its boundary conditions. It is a collection of *influence vectors*, which are successively created for each element of the structure. Every influence vector is composed by storing the response of the whole structure (all elements) due to imposition of a unit virtual distortion in a selected element. Green's functions in *continuum* are the analogy to the influence matrix for discretized (discrete) structures. A detailed description of VDM and its applications can be found in [20].

2.2 VDM-based damage identification

Let us briefly describe the inverse dynamic problem of damage identification, addressed previously in [21], [22]. The objective is to determine damage location and intensity, both specified by the damage vector μ_i, whose components correspond to the assumed discretization of the structure (finite elements). The vector μ_i, is the stiffness degradation ratio (the quotient of the current E_i and initial E'_i Young's modulus) expressed in terms of strains $\varepsilon_i(t)$ and virtual distortions $\varepsilon_i^0(t)$, as follows:

$$\mu_i = \frac{E_i}{E_i'} = \frac{\varepsilon_i(t) - \varepsilon_i^0(t)}{\varepsilon_i(t)} \tag{2.1}$$

Note that the damage vector μ_i is time independent in contrast to strains and virtual distortions.

Let us define the objective function as the mean-square distance f_A between the measured response $\varepsilon_A^M(t)$ and the numerical response $\varepsilon_A(t)$ collected from the sensor locations A. The responses are due to the known excitation $\varepsilon_\alpha^0(\tau)$ generated in the actuator location α. The numerical response is a superposition of the component $\varepsilon_A^L(t)$, expressing an intact response, and the component $\varepsilon_A^R(t)$, adapting the intact response to the measured response $\varepsilon_A^M(t)$, by proper setting of virtual distortions $\varepsilon_j^0(t)$ in possible damage locations j (potentially the whole

structure). The influence matrix D, built at the start of numerical simulation, plays the crucial role in VDM-based modelling. Thus, the objective function is expressed as:

$$f = \sum_A f_A = \sum_A \sum_t \left[d_A(t) \right]^2 , \tag{2.2a}$$

where

$$\begin{aligned} d_A(t) &= \varepsilon_A^M(t) - \varepsilon_A(t) = \varepsilon_A^M(t) - \left[\varepsilon_A^L(t) + \varepsilon_A^R(t) \right] = \varepsilon_A^M(t) - \sum_t \left[\varepsilon_A^L(t) + \varepsilon_A^R(t) \right] = \\ &= \varepsilon_A^M(t) - \sum_{\tau \le t} \sum_{\tau' \le \tau} \left[\sum_\alpha D_{A\alpha}(\tau - \tau') \, \varepsilon_\alpha^0(\tau') + \sum_j D_{Aj}(\tau - \tau') \, \varepsilon_j^0(\tau') \right] . \end{aligned} \tag{2.2b}$$

The inverse dynamic problem of damage identification consists in finding the minimum of the function f with μ_i as design variables. In view of the definition Equation (2.1), the following self-explanatory constraints on μ_i have to be considered:

$$0 \le \mu_i \le 1 \tag{2.3}$$

To solve the optimization problem, a gradient-based approach is applied, with the following analytical gradient calculated from the Equations (2.2):

$$\nabla f_k = \frac{\partial f}{\partial \mu_k} = \sum_A \frac{\partial f_A}{\partial \mu_k} = -2 \sum_A \sum_t d_A(t) \left[\sum_{\tau \le t} \sum_{\tau' \le \tau} \sum_j D_{Aj}(\tau - \tau') \frac{\partial \varepsilon_j^0(\tau')}{\partial \mu_k} \right], \tag{2.4}$$

Transforming Equation (2.1), the relation between the defect parameters μ_i and the virtual distortion $\varepsilon_j^0(t)$ simulating this defect (in the time instance t) is:

$$\sum_j \left[\delta_{ij} - (1 - \mu_i) \, D_{ij}(0) \right] \varepsilon_j^0(t) = (1 - \mu_i) \left[\sum_{\tau \le t} \sum_\alpha D_{i\alpha}(t - \tau) \, \varepsilon_\alpha^0(\tau) + \sum_{\tau < t} \sum_j D_{ij}(t - \tau) \, \varepsilon_j^0(\tau) \right] \tag{2.5}$$

After differentiating Equation (2.5), the partial derivatives $\partial \varepsilon_j^0 / \partial \mu_k$ appearing in Equation (2.4) can be determined from the following:

$$\sum_j \left[\delta_{ij} - (1 - \mu_i) \, D_{ij}(0) \right] \frac{\partial \varepsilon_j^0(t)}{\partial \mu_k} = -\delta_{ik} \, \varepsilon_i(t) + (1 - \mu_i) \sum_{\tau < t} \sum_j D_{ij}(t - \tau) \frac{\partial \varepsilon_j^0(\tau)}{\partial \mu_k} . \tag{2.6}$$

The iterative algorithm for the multi-defect identification requires calculation (from Equations. (2.5) and (2.6)) of the defect-simulating distortions $\varepsilon_j^0(t)$ and their gradients $\partial \varepsilon_j^0 / \partial \mu_k$, for each time step of the Newmark dynamic analysis. Making use of these components, the objective function, Equation (2.2), and its gradients, Equation (2.4), can be calculated. Having determined the gradient of the objective function, the following optimization step is proposed:

$$\mu_i = \mu_i - \frac{\gamma f(\mu_i)}{\nabla f_i^T \nabla f_i} \nabla f_i , \tag{2.7}$$

where γ = const. (reduction coefficient of the objective function value, practically between 0.1 and 0.3) and $f(\mu_i)$ is the current value of the objective function. Then, the calculation of the objective function and its gradients for the modified structure response can be performed in succeeding iterations until the termination criterion is met.

2.3 VDM-based identification algorithm

The VDM-based identification algorithm performs the following steps:

1. Complete modal analysis,
2. Excite the beam with the windowed sine burst (isolated eigenmode providing smooth vibration response),
3. Choose a low (below 1 kHz) eigenfrequency resulting in the highest value of the objective function,
4. Look at initial gradients (rough indication of potential damage locations),
5. Perform optimization:
   a) modify damage coefficient according to Equation (2.7),
   b) take heuristic (not belonging to classical optimization) care of the constraints Equation (2.3).

2.4 VDM settings: dynamic parameters and FE discretization

The cost of computation of the gradients, Equation (2.4), has been discussed in [21]. Quantitative results for a simple beam are presented in Table 3, Section 5. The cost is influenced by the initial parameters assumed in the analysis; especially by the number of time steps in the Newmark algorithm and by extension of the potentially damaged zone of the structure (the numbers of finite elements for which gradients are calculated). A higher number of time steps leads to results that are more accurate. However, a saturation point (due to a tiny step length in the Newmark algorithm) can be determined at a certain stage beyond which no significant improvement is observed. This is the correct compromise between accuracy and computational speed. Computations are slowed considerably when the number of finite elements considered for the potential damage is increased. Therefore, any suggestion on where the damage may be located, based on engineering judgment, is valuable as it narrows the inspection zone. If a small defect is expected, the FE size should roughly correspond to the initial guess otherwise it will not be detected.

2.5 VDM algorithmic improvements: computational time reduction

The idea of the moving window technique is to choose an arbitrary zone of the structure, consisting of fewer elements than the primary number of all elements between the actuator and sensor. The selected window is then moved along between the actuator and sensor, and identification performed. If there is no damage in the part of the structure covered by the moving window, the optimization algorithm will calculate a drop of the objective function by no more than one order of magnitude and will oscillate around the value. The fact that the algorithm cannot perform a further drop of the objective function is interpreted as no damage in the window placed in the current position. A drop by at least three orders of magnitude will be observed if there is damage in the moving window, and is good enough in terms of accuracy and computational time. The advantage of this technique is a significant reduction of computational time (see Table 5, Section 5) because of the limited part of the structure inspected (fewer finite elements). The disadvantage of the technique is that the selected window has to be moved many times in order to cover the whole zone between the actuator and sensor. However, repeating many analyses quickly for large structures should be significantly faster than carrying out a single time-consuming one.

Another technique proposed for the reduction of computational time is automatic selection (using VDM-based software) of a window covering the appropriate zone of damage. An initial window (initial guess) has to be placed somewhere in the structure, but gradients are calculated for all other elements between the actuator and sensor as well. In other words, the main interest is concentrated on the initial window, but the rest of the structure is also monitored (see Figure 5.11). Computational time compared to the moving window technique is increased but the initial window can be moved automatically by analysing negative gradient values in the optimization process. Hence, this analysis does not have to be repeated as in the moving window technique and is competitive in terms of calculation effort.

There is an issue in limiting the identification interest to one major defect. This implies a marked simplification of the algorithm because the influence matrix D is significantly reduced. From Equation (2.2), the one-defect approach leads to elimination of the internal sum over *j* (similarly in Equation (2.4)). In physical terms, this means disregarding the inter-relationship between neighbouring elements and is contrary to the standard VDM approach. As a result, the computations are much quicker, but only one defect can be detected. This approach will be the subject of investigation in future research.

3 CBR-based approach

3.1 CBR vs. soft-computing methods

This section describes a hybrid reasoning system for damage identification [23] developed by the MICE Lab. The system combines a model of the structure with a CBR scheme to evaluate existence of damage and its parameters, location, extension (dimension), and intensity (severity).

Most structural health monitoring methods include Artificial Intelligence, involving: wavelet transformations [24], [25], artificial neural networks [26], [27], genetic algorithms [28], and statistical analysis [29], [30], [31]. However, the use of knowledge-based approaches (such as CBR) has not been exploited specifically for damage detection although it has been suggested by Natke and Yao [32]. In the field of structural design, some researchers have applied CBR to bridge design [33]. Since many modelling possibilities exist to explain the behaviour of structures, Raphael and Smith [34] describe an approach for selecting appropriate causal models for engineering diagnosis.

The structural dynamic responses to given excitations are simulated in the presence of different forms of damage using one or more models. A collection of the responses forms a set of *cases*. In a *learning mode*, an initial *casebase* is created using Self-Organizing Maps (SOM) as a classification tool [35]. To reduce the number of input signals to SOM without reducing the classification accuracy required, the Wavelet Transform (WT) [36], [37] is used to extract features from the measured signal while retaining most of the intrinsic information. When the system is working in its *operating mode*, data acquired by sensors are used to perform a diagnosis by analogy with the cases stored in the casebase, reusing and adapting old situations (see Figure 3.1). Whenever a new situation is detected, it is retained in the casebase in order to update the available information.

3.2 Cases

A case is “a contextualized piece of knowledge representing an experience that teaches a lesson, fundamental to achieving the goals of the reasoner” [38]. In the problem of damage assessment,

each case is a register, which contains information about the defect in the structure (location, dimension, and severity) and the minimal representation of the simulated dynamic response.

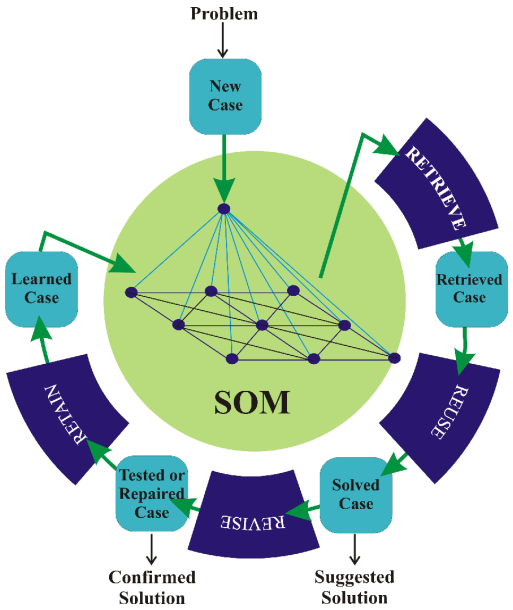

Figure 3.1 Proposed CBR cycle

3.3 Casebase building

A casebase is an array in memory organizing all cases to facilitate the search for the case most closely matching the current problem. In the presented methodology, each casebase is an SOM. The minimal representation is a set of principal features that are extracted from the coefficients of the Wavelet Transform applied to the simulated dynamic response. Figure 3.2 shows the process of feature extraction and of building a casebase.

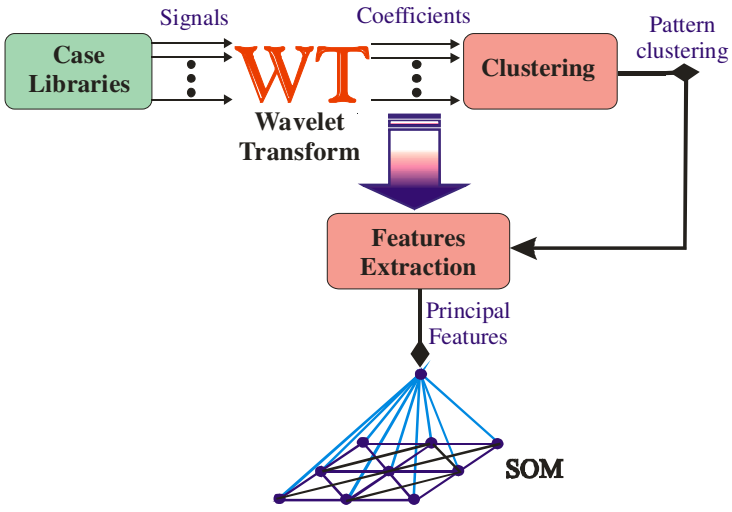

Figure 3.2 Casebase building

To extract the principal features, the wavelet coefficients are computed for each selected case. The coefficients at the same position in different cases are considered as samples of independent

random variables. Therefore, from the Central Limit Theorem, each variable is approximately normally distributed. The mean values of the Gaussian distribution and the maximal wavelet coefficients occur at the same positions, which determine the midpoints of clusters. This pattern of clusters contains relevant signal information. Subsequently, each feature is determined as the square root of the energy of the wavelet coefficients in the corresponding cluster [39].

After the cases are generated, they are organized in memory for recovery at the required time. An SOM is created and trained. It has *l* neurons (one for each feature) in the input layer and *m*n* (*m* and *n* depend upon the number of cases to store) clusters (or neurons) in the output layer. The network organizes the cases with similar characteristics in each cluster.

3.4 Retrieving

Checking the methodology or putting the system in the operating mode can be performed by numerical simulation, laboratory testing, or in normal working conditions for real structures. The dynamic response of a damaged structure is collected. From the response signal, the principal features are extracted using the clustering pattern previously defined. From these features, the SOM retrieves a set of previously stored cases with similar characteristics. Table 1 presents an example of the cases (dimension and severity) retrieved from the activated clusters together with their distances from the analysed new case.

Table 1 CBR: An example of the retrieved cases

Damaged element (dimension)	Severity	Distance
15	30%	0.00362
14–15	10%–10%	0.00747
11–14–15	10%–10%–10%	0.01123
11–15	10%–10%	0.01483
11–14	15%–15%	0.01517

3.5 Adapting

Among the retrieved cases, we want to reward: i) elements that are repeated several times—the more frequent the repetition, the higher the probability of being the *winner*—and ii) similar cases—the smaller the distance, the higher the probability of being the winner. To this end, a factor is calculated for each element, which is the sum of distance reciprocals over the cases in which the element is present. For example, the factor for the Elements 11, 14, and 15 are:

$$\begin{aligned} F_{11} &= \frac{1}{0.01123} + \frac{1}{0.01483} + \frac{1}{0.01517} = 222.40 \\ F_{14} &= \frac{1}{0.00747} + \frac{1}{0.01123} + \frac{1}{0.01517} = 288.84 \\ F_{15} &= \frac{1}{0.00362} + \frac{1}{0.00747} + \frac{1}{0.01123} + \frac{1}{0.01483} = 566.59 \end{aligned} \tag{3.1}$$

By normalizing these factors, the probabilities of damage in each element are calculated (Element 15 has probability 1, Element 14 probability 0.51, and Element 11 probability 0.39, in the presented example). To calculate the dimension and severity of defects, a weighted average is computed, using the weighting coefficients presented in Equations (3.2), where *n* is the total number of retrieved cases, *dim*, *sev,* and *d* are the dimension, severity, and distance of each retrieved case, respectively. Note that *d(1)* is the minimum distance. In the presented example,

the dimension is 1.7, rounded to two elements (Elements 15 and 14), and the severity is 26.8% (stiffness reduction).

$$\text{Dimension} = \sum_{j=1}^{n} \dim(j) * \frac{d(1)/d(j)}{\sum_{i=1}^{n} d(1)/d(i)}$$
$$\text{Severity} = \sum_{j=1}^{n} \text{sev}(j) * \frac{d(1)/d(j)}{\sum_{i=1}^{n} d(1)/d(i)} \quad (3.2)$$

3.6 CBR-based identification algorithm

The CBR-based identification algorithm performs the following steps:
Learning mode

a. Choose a structure to study,
b. Define what damage parameters are to be identified (location, dimension, severity),
c. Choose a set of cases that contain previous simulations of several structural damage scenarios,
d. Build a casebase from the selected cases.

Operating mode

a. Load the waveform detected by the sensor during the test of the selected structure,
b. Retrieve the similar cases from the casebase,
c. Adapt the previous solutions to propose a new solution,
d. Generate the outcome report and display the damage of the structure,
e. Retain the new solution as part of a new case once it has been confirmed or validated.

3.7 CBR settings: representative casebases

Representative casebases need to be built to get a meaningful identification result using CBR. This means that a casebase should correspond to the expected type of damage as far as the number of damage locations, and their extension and intensity are concerned. A properly built casebase, reflecting the features of a real defect, will enhance the quality of the identification results. The number of cases stored in a casebase influences quality, but also computational time. However, a saturation point occurs, similar to that in the time steps in the VDM approach (see Section 2.4). Credibility of a casebase should be assured by proper calibration of the numerical model used for generation of cases of damaged structure responses. This issue is addressed in the next section.

4 Model calibration

Model calibration has to be performed for the VDM-based approach, which is a model-updating method of damage assessment. The CBR-based approach also uses a numerical model to generate responses of damaged structures while building a casebase. Thus, model calibration is an important stage of the analysis, which should be done as accurately as possible in order to enable successful damage identification.

4.1 Specimen description

Model calibration is demonstrated for an aluminium cantilever beam, 98 cm long, 2 cm wide, and 0.5 cm high, tested in the STC laboratory. The beam was excited with the piezo-actuator (Figure 4.1a) mounted close to the clamped end. The piezo-patch sensor (Figure 4.1b) close to the free end collected the response.

A numerical model of the specimen was created. The model consists of 49 beam elements of 2 cm length each. Two beam parameters need to be tuned to match the experimental response, Young's modulus and density. Analogous parameters for the steel mountings (the two small plates screwed to the beam in Figure 4.1a) and the actuator (the ellipse in Figure 4.1a) were assumed to be constant. The piezo-patch sensor has been disregarded in modelling, as its thickness (together with the glue) and mass are negligible.

Figure 4.1 Actuator and sensor mounted on the beam

4.2 Excitation signal

The structure in the PD project was excited with a frequency corresponding to a selected eigenmode range, from the 1st to the 20th eigenmode of the structure. The low frequency range favours a moderate numerical cost, as dense sampling of the signal is not required. In addition, long-distance propagation of the excitation signal is assured using low frequencies for which dispersion is low. The high frequency range is preferred for detection of a relatively small defect (the ratio of damage extension to the applied wavelength should be no smaller than 5%). The choice of excitation frequency is always a compromise between the above-mentioned factors.

At the beginning of the PD project, a pure sine pulse was used as the excitation signal. Subsequently, a windowed sine burst (widely used in the Wavelet Transform) was found to be more effective in inducing the required vibration mode. The windowed sine burst used by the PD software is expressed by the equation:

$$\mathrm{Exc}(t) = n * \arcsin\left(\sin\left(\frac{1}{n} 2\pi f t\right)\right)\sin(2\pi f t) \qquad (4.1)$$

where n is the number of sine half-cycles enclosed in the window and f is the excitation frequency. There is one dominant frequency in the Fast Fourier Transform for the windowed burst, whereas the spectrum for the pure sine pulse comprises some side-frequencies. Consequently, the response of the structure excited by the windowed sine burst is smooth (cf. Figures 4.2 and 4.3) and stabilizes quickly resembling a steady state, whereas the pure sine pulse response is rough and unsteady (cf. Figures 5.2, 5.3, and 5.6).

The 2.5-cycle and 4.5-cycle windowed sine pulses were used for excitation. The shapes of the excitation signals and corresponding responses are shown in Figures 4.2 and 4.3. The applied frequency corresponds to the 7th eigenfrequency of the beam, which is 491 Hz. The dynamic response is calculated by the Newmark algorithm in 2500 time steps, 1.018e–02 m each.

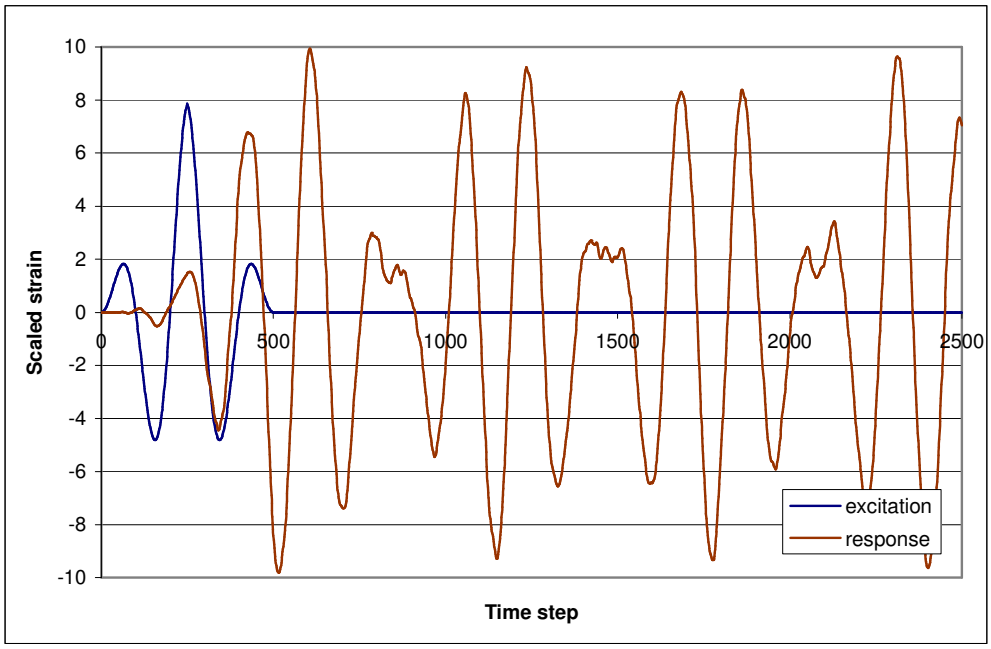

Figure 4.2 The 2.5-cycle windowed sine bursts and corresponding response

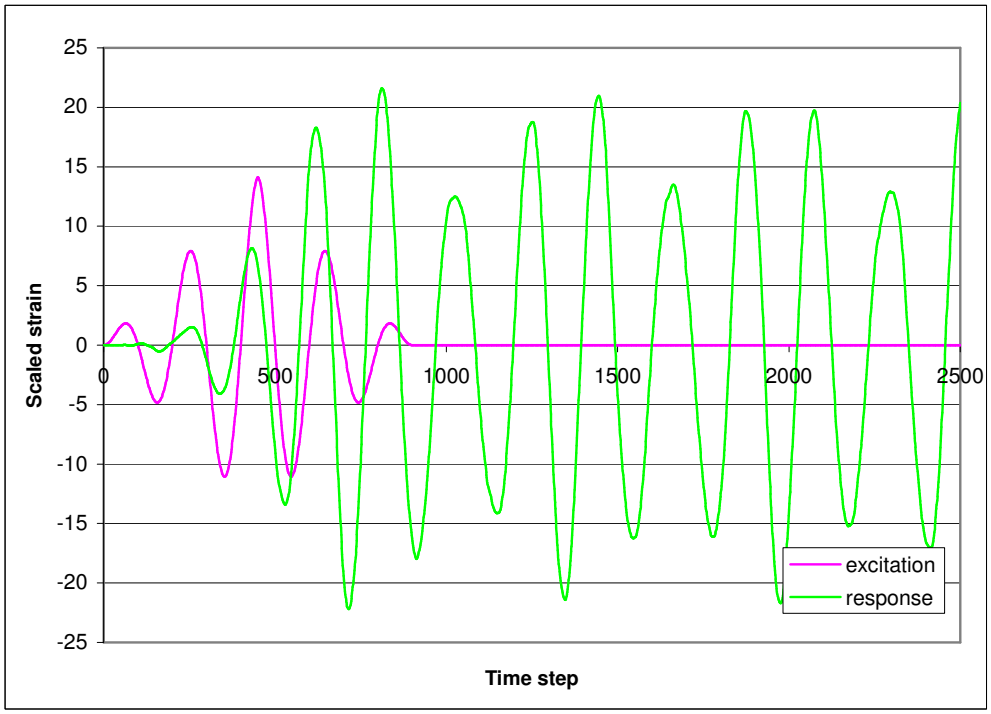

Figure 4.3 The 4.5-cycle windowed sine bursts and corresponding response

4.3 Results for the undamaged structure

Selection of the best parameters for matching the experimental and numerical responses was carried out with the help of the mean square error (MSE) surface presented in Figure 4.4. The mean square error is shown on the vertical axis of the plot depending on the Young's modulus and density of aluminium as the parameters of modification (horizontal plane). The best parameters (producing the least error) for aluminium were E = 65.8 GPa, ρ = 2690 kg/m^3, as shown on the MSE surface. The parameters of the actuator zone were fixed during the calibration (E = 28 GPa, ρ = 7200 kg/m^3 for the ellipse and E = 207 GPa, ρ = 7800 kg/m^3 for the mounting steel—see Figure 4.1a).

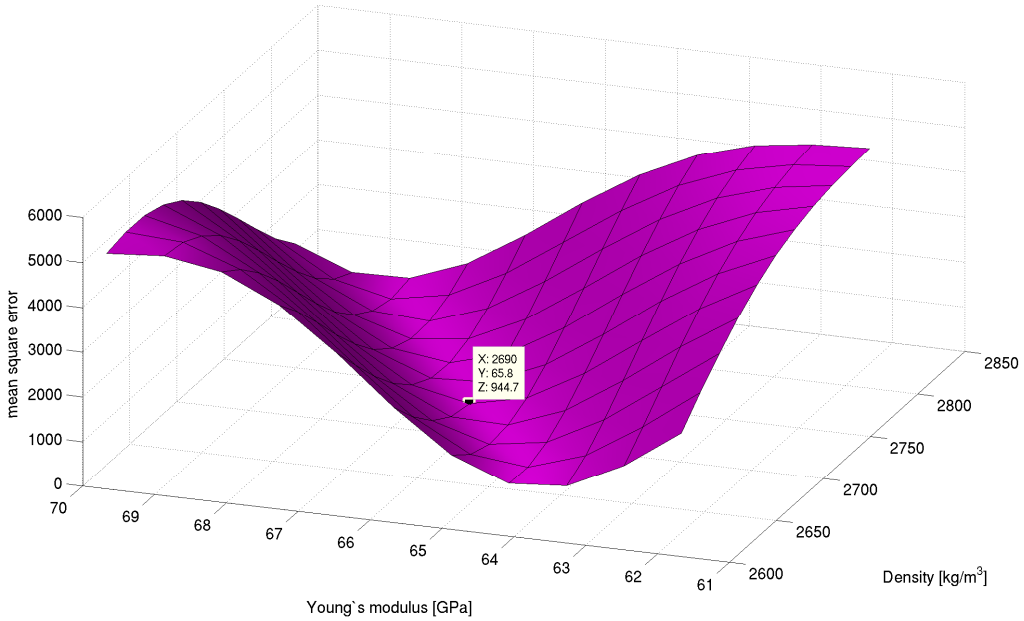

Figure 4.4 Mean square error surface for determining optimal material parameters for the beam

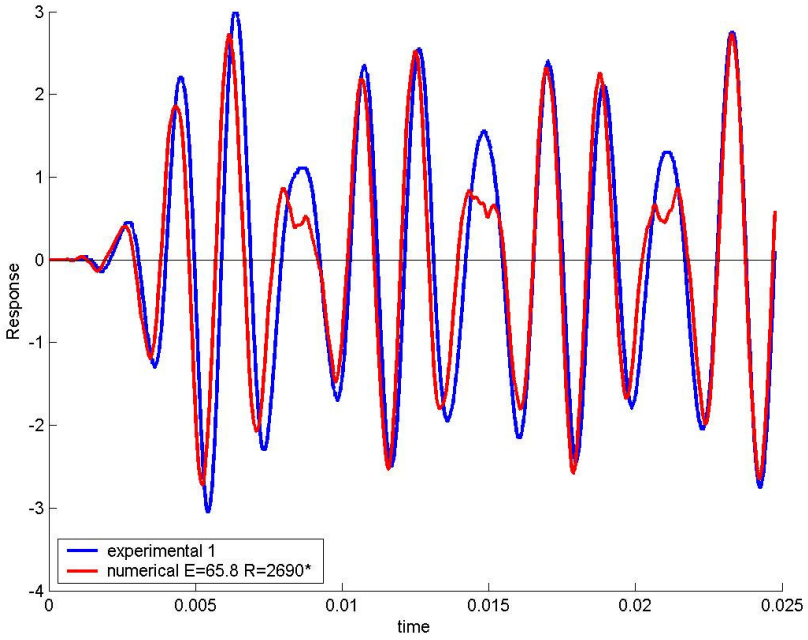

Figure 4.5 Numerical vs. experimental response for the beam excited with the 2.5-cycle sine burst

Comparison between the experiment and the numerical calculations for optimally selected parameters is demonstrated in Figure 4.5. The numerical response is not smooth in three places and matching can be still improved.

The fluctuations of the numerical response, clearly observed in three places in Figure 4.5, provided the incentive to look for a better match. Therefore, another shape of the excitation signal was used consisting of 4.5 cycles in the enveloping window. As shown in Figure 4.6, the fluctuations were eliminated in the numerical response and the agreement with the experiment was much better.

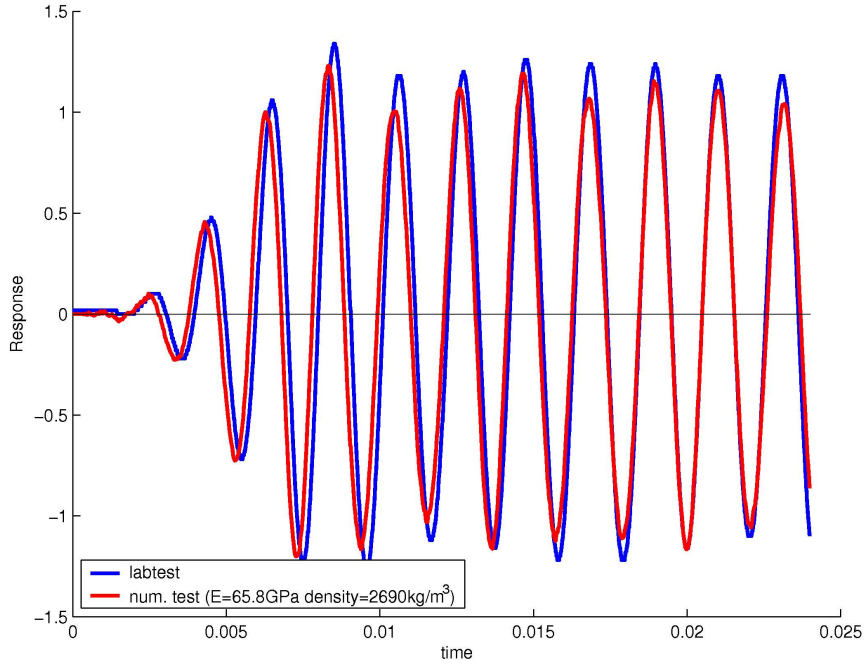

Figure 4.6 Numerical vs. experimental response for the beam excited with the 4.5-cycle sine burst

5 Numerical example of a beam

This section presents numerical calculations for the beam specimen described in Section 4. Demonstration of the complexity of the inverse problem, solved using the VDM approach, is provided first in [40]. The results of the two approaches are then compared. Damage identification results are presented qualitatively and the required computational times are presented quantitatively.

5.1 Demonstration of the complexity of the inverse problem

Inverse problems are complex by nature [41]. Some of their intrinsic features influencing the effectiveness of the VDM-based software are demonstrated here. Let us consider two configurations (shown in Figure 5.1) of the cantilever beam (described in Section 4) subjected to damage. The actuator and sensor are equidistant from the beam edges. The inspected zone between the actuator and sensor comprises 23 finite elements.

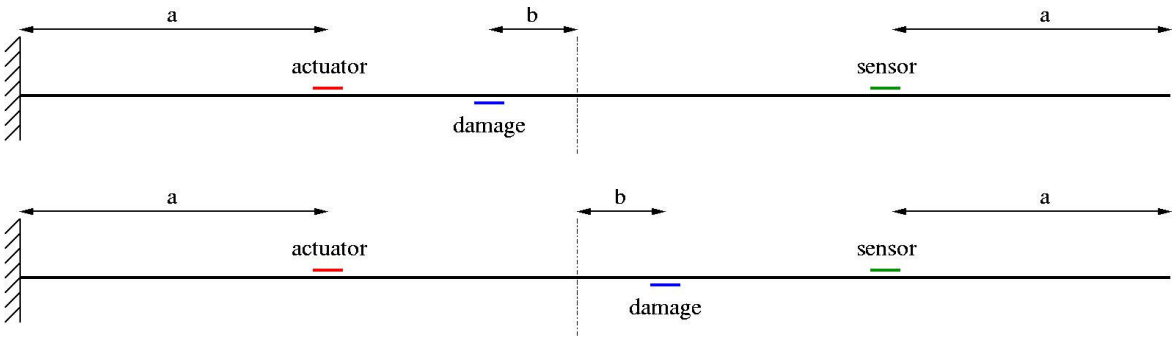

Figure 5.1 Two configurations of a cantilever beam subjected to damage

The beam model is idealized by disregarding the mass of the actuator. The applied excitation is a sine pulse of frequency corresponding to the 7th anti-symmetric eigenmode (see Figure 5.7). The transient responses of the beam, with damage located symmetrically around its middle axis, are identical (see Figure 5.2) even though the boundary conditions and the eigenmode are not symmetrical. This numerical result is intriguing and requires in-depth investigation not considered here.

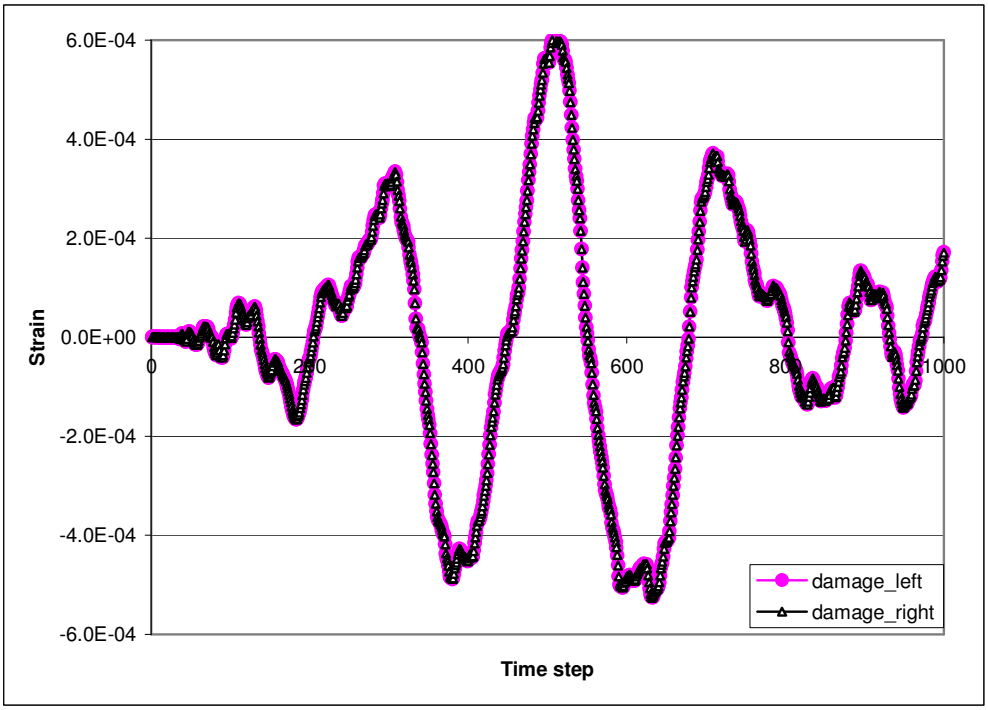

Figure 5.2 Two identical responses of the idealized beam (non-uniqueness)

The direct implication of the problem of non-uniqueness is that the damage identification algorithm cannot distinguish between the two cases of symmetrical damage configuration (cf. Figure 5.1) for the idealized beam. The algorithm processes such a case, but the produced solution will always include true and false damage locations (see Figure 5.3).

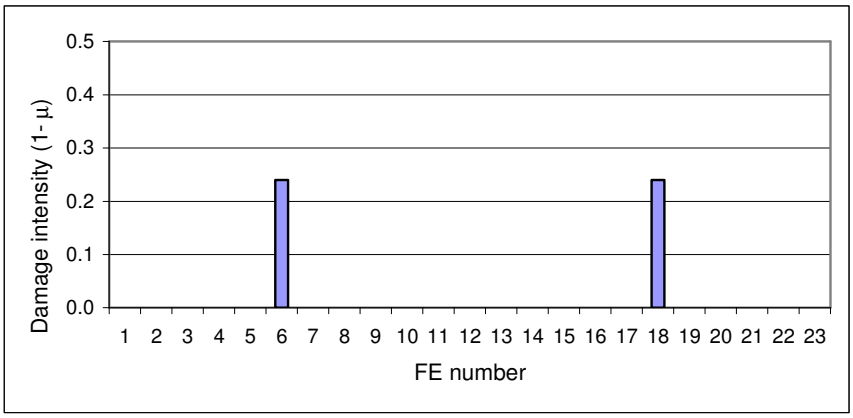

Figure 5.3 Damage identification for the symmetrical damage configuration (true damage in el. 6 of intensity 0.5)

To avoid the coincidence of responses depicted in Figure 5.2, the actuator and sensor should not be placed equidistant from the edges or perturb the symmetry of the model, for example by using an added mass. For instance, if we account for the mass of the actuator, which was approximately 16% of the beam mass, the transient responses become clearly distinguishable, as demonstrated in Figure 5.4.

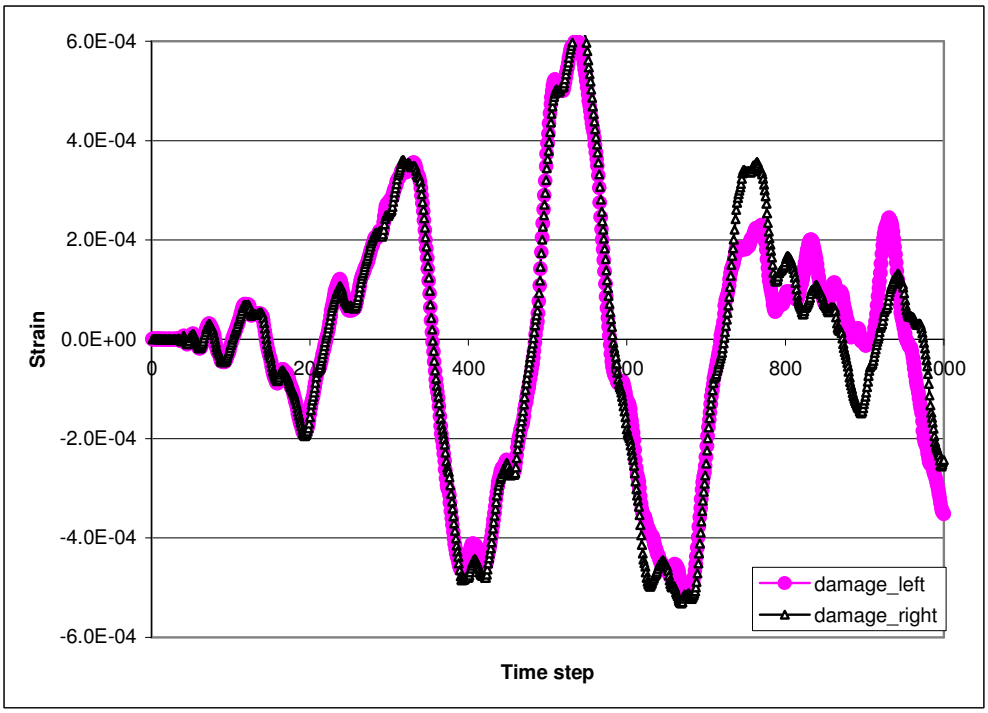

Figure 5.4 Two distinguishable responses of the actual beam with included mass of the actuator

The fact that the objective function, Equation (2.2), exhibits many local minima makes the inverse problem difficult to solve. To demonstrate this, let us consider two kinds of damage applied to the beam. In Figure 5.5a, distributed damage (extending over five finite elements) is depicted, whereas in Figure 5.5b, concentrated damage (corresponding to one finite element) is depicted.

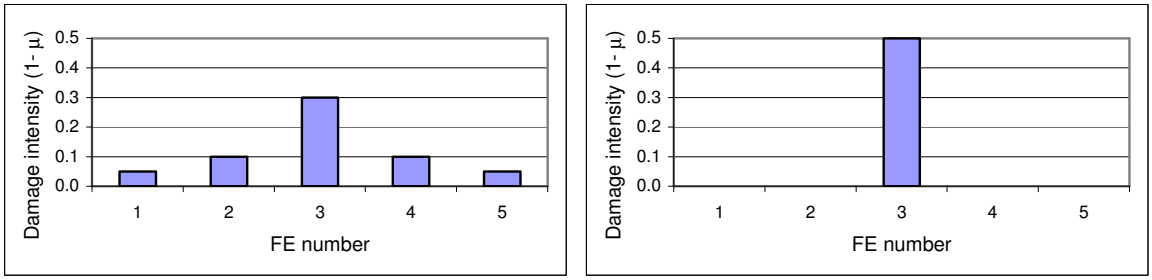

Figure 5.5 Distributed vs. concentrated damage

It is difficult to observe the difference in responses of the beam to the two kinds of damage (see Figure 5.6), which makes the two cases difficult to distinguish for the identification algorithm.

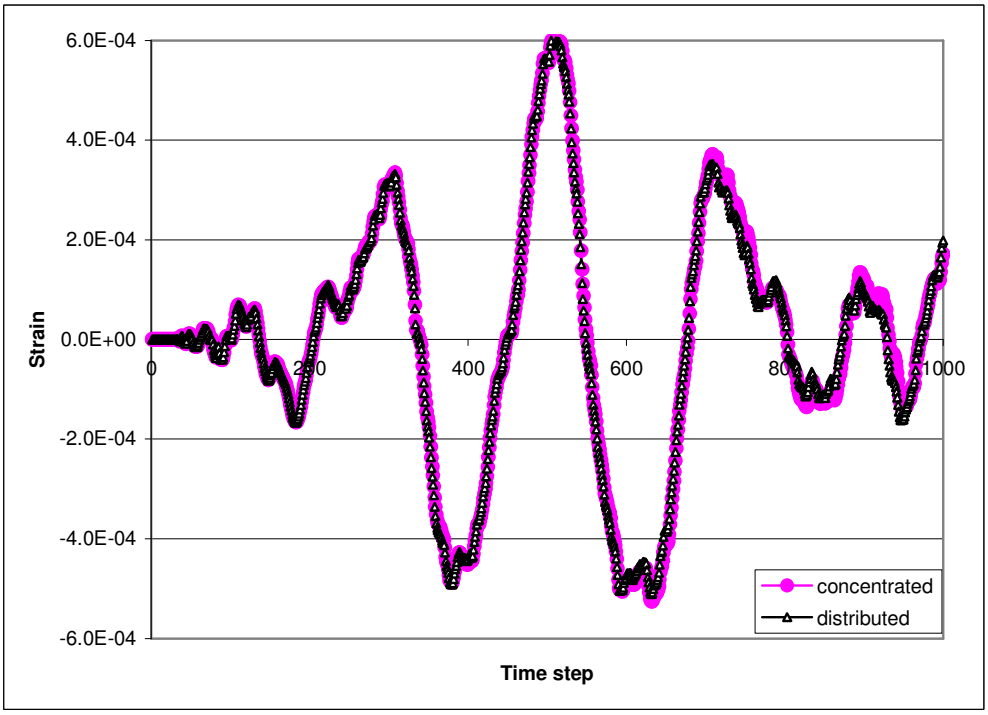

Figure 5.6 Two close responses of the beam to two kinds of damage (local minima)

5.2 Comparison of the effectiveness of the two approaches

The cantilever beam structure, described in Section 4, was chosen to demonstrate the effectiveness of the PD software. The actuator was mounted in the middle of the beam (see Figure 5.7) to avoid the problem of false damage identification (see Section 5.1). The beam was excited with the 2.5-cycle windowed sine burst (cf. Equation (4.1)) of frequency 491 Hz, corresponding to the 7th eigenmode.

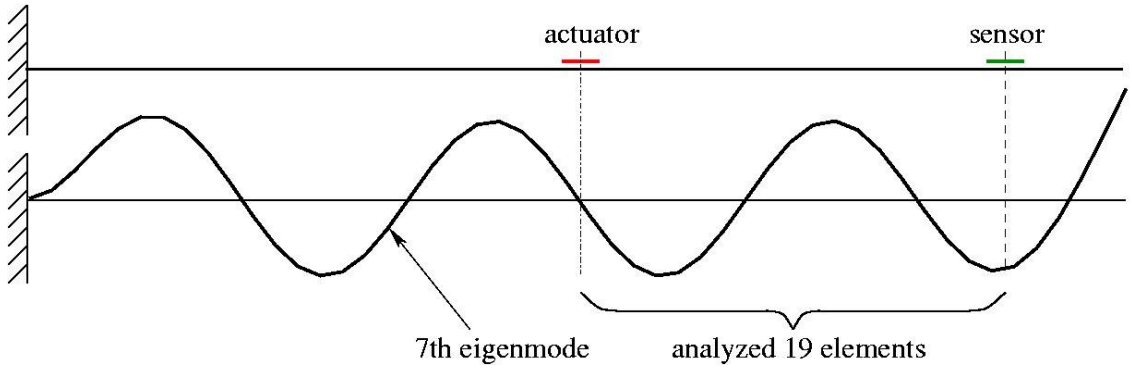

Figure 5.7 Cantilever beam analysed using VDM and CBR

The zone between the actuator and the sensor, comprising 19 elements, was inspected. The damage in the structure was simulated numerically by reduction of Young's modulus in selected finite elements. Three damage cases, summarized in Table 2, were considered.

Table 2 Assumed damage cases

Element chosen as damaged	Damage intensity coefficient (1–μ)		
	Damage Case 1	Damage Case 2	Damage Case 3
Element No. 5	0.0	0.3	0.3
Element No. 10	0.0	0.0	0.2
Element No. 15	0.5	0.5	0.5

Table 3 shows computational times for obtaining a solution using the VDM-based identification procedure for each damage case. Reduction of the objective function by orders of magnitude occurred in the gradient-based optimization process. It is clear that a more accurate solution requires more time. The VDM-based computations were accomplished using a PC equipped with a 3.0 GHz processor.

Table 3 Computational times for VDM

VDM objective function	Computational time [m]		
	Damage Case 1	Damage Case 2	Damage Case 3
Drop by 1 order	12	15	16
Drop by 2 orders	89	72	69
Drop by 3 orders	327	444	283
Drop by 4 orders	947	1019	760

Table 4 shows analogous computational times for the CBR-based identification procedure. The constructed casebases were as follows:

- Casebase I (one defect): 127 structural responses of simulated defects in a single element between the actuator and sensor with a thickness reduction of 10%, 20%, 30%, 40%, 50%, and 60%.
- Casebase II (two defects): 630 structural responses of simulated defects in two separated (possibly neighbouring as a special case) elements between the actuator and sensor with a thickness reduction of 10%, 30%, and 50%.
- Casebase III (three defects): 1336 structural responses of simulated defects in three separated elements between the actuator and sensor with a thickness reduction of 10%, 30%, and 50%.

It is evident that the number of cases in a casebase influences computational time. The CBR-based computations were accomplished using a PC equipped with a 2.4 GHz processor.

Table 4 Computational times for CBR

CBR Casebase	Computational time [m] for all damage cases		
	Library building	Training	Total
Casebase I	1.4	0.1	1.5
Casebase II	6.5	2.0	8.5
Casebase III	12.5	4.8	17.3
Casebase I + II	7.9	1.7	9.6
Casebase I + II + III	20.5	19.9	40.4

Evolution of damage is presented for the Damage Case 1 in Figure 5.8, identified by VDM in four stages (increasing accuracy) corresponding to reduction of the objective function by one order of magnitude. The damage intensity coefficient (1–μ) obtained directly from the gradient-based optimization is depicted on the vertical axis.

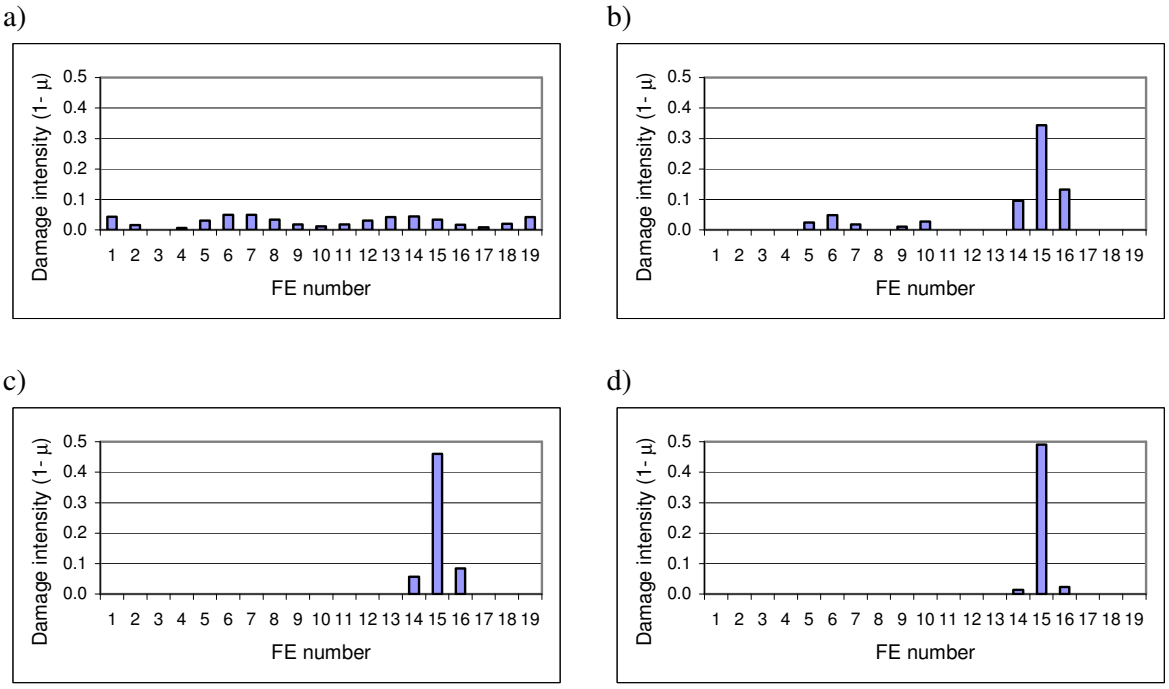

Figure 5.8 Damage evolution by VDM for Damage Case 1, objective function drop: a) by 1 order, b) by 2 orders, c) by 3 orders, d) by 4 orders

Analysis of the VDM damage evolution charts leads to the conclusion that the drop of the objective function by only one order of magnitude is not informative as all three damage cases look virtually the same. The drop of the objective function by three orders of magnitude (Figure 5.8c) is the most suitable point at which identification should be terminated. The results give satisfactory identification quality and are affordable in computational time.

Figure 5.9 shows the results of damage identification using VDM for the Damage Cases 2 and 3 with an objective function drop of three orders of magnitude as the termination criterion for the optimization algorithm.

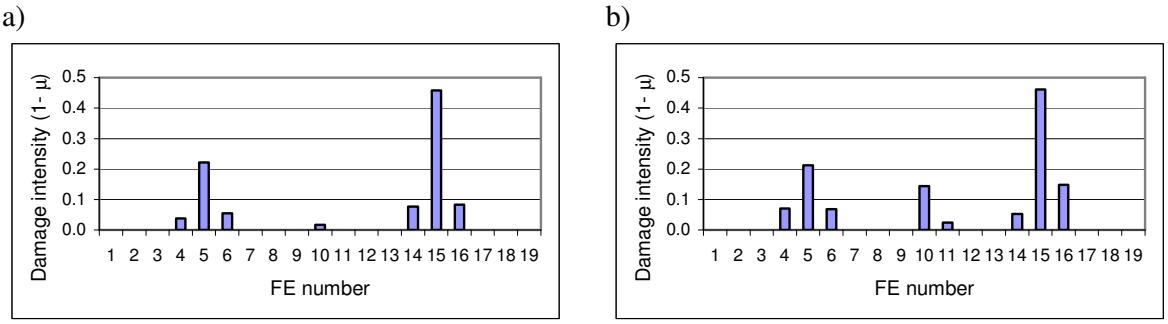

Figure 5.9 Damage identification using VDM: a) Damage Case 2, b) Damage Case 3

The damage identification results using CBR are shown in Figure 5.10 according to the type of casebase used and the type of defect detected. In Casebase I, containing cases of only one defect between the actuator and sensor, the correct location of the Damage Case 1 was found. Similarly, for Casebase II grouping cases of two simultaneous defects, two defects as in the assumed Damage Case 2 were detected correctly. An analogous conclusion holds for Casebase III. For the single casebases (Casebase I, II, or III), the results are good. However, a serious limitation is that the user should know the number of defects in advance to use the proper casebase. Thus, an identification of two defects with Casebase I or III is not applicable, as there is no case of two defects in these casebases. An alternative for single casebases is the use of combined casebases (e.g., Casebase I + II, I + II + III). For instance, with Casebase I + II + III, we can perform identification of all assumed damage cases. However, the quality of results is worse. In other words, single casebases (special purpose) detect a certain damage pattern with good accuracy, whereas combined casebases (general purpose) detect various damage patterns but with less accuracy.

The vertical axis in Figures 5.8 and 5.9 shows the damage intensity coefficient (1–μ) for VDM plots while the vertical axis in Figure 5.10 shows the probability of damage location for CBR plots. Therefore, the graphs cannot be compared directly. To determine the severity of damage with CBR, it is necessary to follow the adapting procedure described in Section 3.5.

The computational times favour CBR (cf. Tables 3 and 4) and are enhanced by using a 2.4 GHz processor in CBR vs. a 3.0 GHz processor in VDM. However, the time reduction techniques for VDM, proposed in Section 2.5, brought significant savings. Computational times using the VDM improvement techniques (shown in Table 5) are comparable to those for the CBR approach (cf. Table 4).

	Damage Case		
Casebase	1	2	3
I	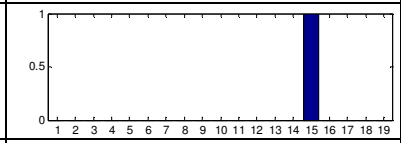	Not applicable	Not applicable
II	Not applicable	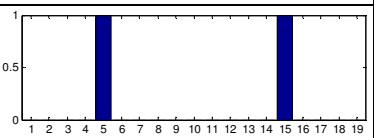	Not applicable
III	Not applicable	Not applicable	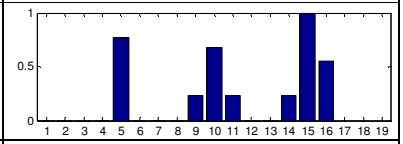
I + II	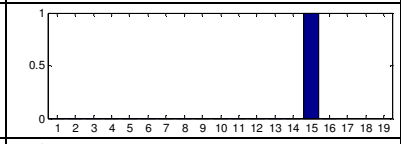	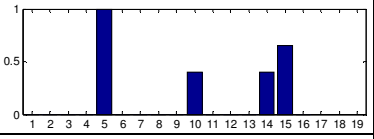	Not applicable
I + II + III	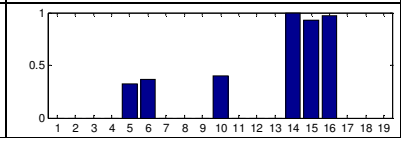	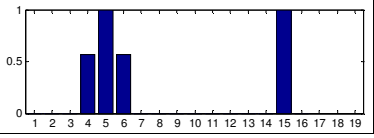	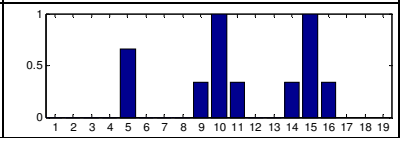

Figure 5.10 Damage identification results using CBR

Table 5 Computational times for VDM improvement techniques

VDM objective function	Computational time [m]–Damage Case 1	
	Moving window	Automatic window
Drop by 1 order	0.7	3.0
Drop by 2 orders	2.5	9.0
Drop by 3 orders	10.0	24.5

Figure 5.11 depicts a history of identification for Damage Case 1 making use of the automatic window technique, which has been proposed to reduce the computational time in the VDM-based approach. The initially selected window comprising seven elements (Elements 1–7) does not include the damaged element (Element 15). After less than ten optimization steps, on the basis of gradient values, a decision was taken to move and split the initial window into two zones (Elements 7–9 and Elements 14–17). It was observed that the true damage (Element 15) tends to dominate as the identification process progresses.

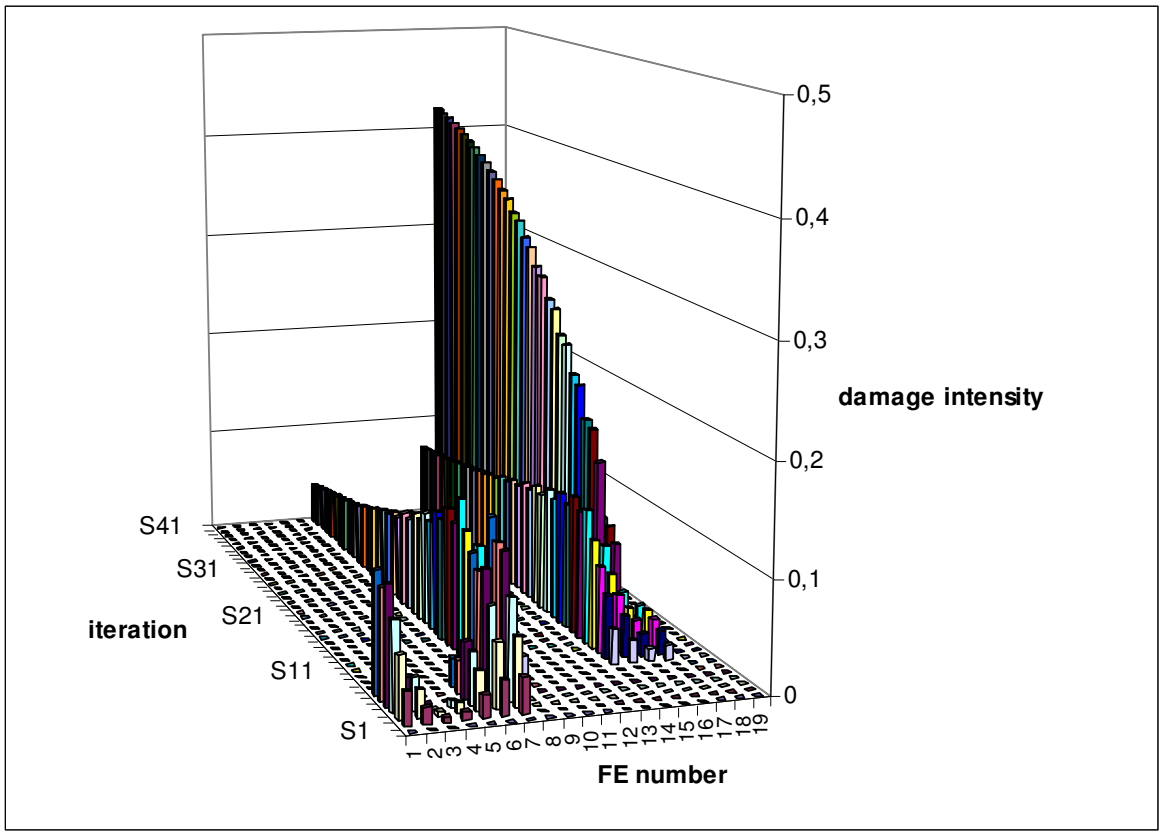

Figure 5.11 Illustration of the automatic window technique for VDM

6 Final remarks

Two damage identification approaches, developed during the PD project, have been described in the paper.

The first task in using these approaches is calibration of the numerical model to experimental results. In general, calibration may be influenced by many factors (e.g., actuator, sensor, excitation, boundary conditions) and can be time-consuming. The parameters, which are the subject of the calibration, are material characteristics such as Young's modulus, density, Poisson's ratio, and damping coefficients. Model calibration has to be completed with satisfactory accuracy. The chances of successful damage identification are radically diminished if a discrepancy between experimental and numerical results is evident.

The VDM-based damage identification method tackles an inverse problem, which is quite complex in nature including non-uniqueness of solution and many local minima of the defined objective function. Therefore, the solution may be difficult to interpret.

The problem investigated was identification of stiffness-impairing (corrosion-like) damage in engineering structures by examining perturbations in vibration responses, induced by piezo-actuators and captured by piezo-sensors. From the PD software point of view, there are two critical factors, which strongly influence the success of the identification process, namely FE discretization and excitation. Discretization must be a compromise between the extension of damage (the more finite elements the better) and the computational time involved (the fewer

finite elements the better), which may be quite long for densely discretized structures. The applied frequency of excitation must also be a compromise in order to assure long-distance propagation (low frequency preferred) on one hand and identification of small defects (high frequency preferred) on the other. The windowed sine burst (cf. Equation (4.1)) produced a smooth, steady-state-like dynamic response.

Two alternative approaches were developed in the PD project. One approach developed by the STC, uses VDM for modelling damage and standard optimization techniques for identifying it. The defined objective function—a mean square strain measure—is minimized in the optimization process. This approach can be classified as a model-updating method solving an inverse dynamic problem in the time domain. The VDM-based approach operates on strains, which may be directly measured, for example by the glued piezo-patches. The identification results are always presented in a deterministic manner. The advantage of the VDM approach is its relatively high accuracy of identification (having in mind the complexity of the inverse problem). The drawback of the approach is the high numerical cost involved due to time-consuming calculation of the objective-function gradients. Some ideas on reduction of cost have been presented in Section 2.5.

The alternative approach developed by the MICE Lab uses CBR for damage identification. The elaborated software package may be described as an efficient data processing tool. The CBR-based approach requires numerous inputs in terms of structural responses in order to create a library (casebase) of various damage cases. It utilizes a soft-computing method (neural network in the form of a self-organizing map) for training the casebase. A new case is identified based on previously stored and trained data. The identification results are always presented in terms of probability. The advantage of the CBR approach is that once the library of cases is built, identification of a new case is almost immediate, whereas with the VDM approach the identification for a new case implies starting the procedure from scratch. The disadvantage of the CBR approach is that the quality of solution is highly influenced by the choice of a proper casebase. If the real number of damage locations is known (rarely the case) and matched with the proper casebase, the identification result will be accurate. Only a rough defect indication will be given when a combined casebase not focused on a certain defect type is used (Figure 5.10). The CBR approach will process data regardless of their physical relevance; it will find a solution even for input signals that have unclear physical interpretation. A vague input (e.g., from experiment), which has not been confronted with a numerical model, will produce a vague output. In practice, it is hard to imagine feeding the CBR procedure with damage cases generated otherwise than by a numerical model. Creating a casebase through experiment is inefficient and costly.

Both methods may be combined where repeated health monitoring of the same part of a structure occurs. The CBR approach should be used first, as it has the advantage of quick identification (case retrieving and adapting) because of the representative library of cases built at the commencement of monitoring. The CBR result may not be very accurate, but will be satisfactory for industrial needs. It can be subsequently refined using the VDM approach if necessary. In non-recurrent health monitoring, the advantage of quick identification by the CBR is lost (the analysis will not be repeated) and the VDM approach appears to be more accurate.

The problem of model calibration appears to be critical for the effectiveness of the proposed PD software. For small demonstrators (e.g., the presented beam), the model calibration is good enough to start damage identification (see Figure 4.6). However, it is a complex task for real structures. The high numerical cost of performing the identification algorithm for large structures

consisting of thousands of finite elements arises with both VDM and CBR. However, fast progress in computer power improvement suggests that computational cost is unlikely to be the major obstacle for the developed PD software. The damage identification methodology described in this paper can be successfully applied to structures modelled by beams, for which the above-mentioned problems do not hold. It may be possible to apply the methodologies to plate and shell structures in the future.

Acknowledgement

This work was financially supported by the 5FP EU Growth Project No. G1RD-2001-00659–PIEZODIAGNOSTICS–Smart Structural Diagnostics using Piezo-generated Elastic Waves; partners: CEGELEC, TWI, ATKINS, CEDRAT, CDRiA, CIMNE, IFTR, ECL, ALSTOM.

References

[1] Rose J. L. (1999) *Ultrasonic waves in solid media*, Cambridge University Press, Cambridge

[2] Muravin G. (2000) *Inspection, diagnostics and monitoring of construction materials by the acoustic emission methods*, Minerva Press, London

[3] Mallet L., Lee B. C., Staszewski W. J., Scarpa F. (2004) Structural health monitoring using scanning laser vibrometry: II. Lamb waves for damage detection, *Smart Materials and Structures*, vol. 13(2), pp. 261–269

[4] Biemans C., Staszewski W. J., Boller C., Tomlinson G. R. (2001) Crack detection in metallic structures using broadband excitation of acousto-ultrasonics, *Journal of Intelligent Material Systems and Structures*, vol. 12(8), pp. 589–597

[5] Staszewski W. J. (2003) Structural Health Monitoring using Guided Ultrasonic Waves, in: *Advances in Smart Technologies in Structural Engineering*, J. Holnicki-Szulc, C. A. Mota Soares (Eds.), Springer, pp. 117–162

[6] Yang S. M., Lee G. S. (1999) Effects of Modeling Error on Structure Damage Diagnosis by Two-Stage Optimization, *Structural Health Monitoring 2000*, Stanford University, Palo Alto, California, pp. 871–880

[7] Ettouney M., Daddazio R., Hapij A. (1999) Optimal Sensor Locations for Structures with Multiple Loading Conditions, *Smart Structures and Materials 1999: Smart Systems for Bridges, Structures, and Highways*, Proceedings of SPIE, Vol. 3, 671, pp. 78–89

[8] Williams E. J., Messina A. (1999) Applications of the Multiple Damage Location Assurance Criterion, *Damage Assessment of Structures*, Proceedings of the International Conference on Damage Assessment of Structures (DAMAS'99), Dublin, Ireland, pp. 256–264

[9] Ho Y. K., Ewins D. J. (1999) Numerical Evaluation of the Damage Index, *Structural Health Monitoring 2000*, Stanford University, Palo Alto, California, pp. 995–1011

[10] Zhang L., Quiong W., Link M. (1998) A Structural Damage Identification Approach Based on Element Modal Strain Energy, *Proceedings of ISMA23, Noise and Vibration Engineering*, Leuven, Belgium

[11] Worden K., Manson G., Allman D. (2001) An Experimental Appraisal of the Strain Energy Damage Location Method, *Damage Assessment of Structures*, Proceedings of the International Conference on Damage Assessment of Structures (DAMAS'01), 25–28 June, Cardiff, UK, pp. 35–46

[12] Fritzen C.-P., Bohle K. (2004) Damage Identification using a Modal Kinetic Energy Criterion and "Output-Only" Modal Data–Application to the Z24-Brigde, P*roc. of the 2nd European Workshop on Structural Health Monitoring*, 7–9 July, Munich, Germany, pp. 185–194

[13] Fritzen C.-P., Bohle K. (1999) Identification of Damage in Large Scale Structures by Means of Measured FRFs-Procedure and Application to the I40-Highway Bridge, *Damage Assessment of Structures*, Proceedings of the International Conference on Damage Assessment of Structures (DAMAS'99), Dublin, Ireland, pp. 310–319

[14] Maeck J., De Roeck G., (2003) Damage assessment using vibration analysis on the Z24 bridge, *Mechanical Systems and Signal Processing*, 71(1), pp. 133–142

[15] Teughels A., De Roeck G. (2004) Structural damage identification of the highway bridge Z24 by FE model updating, *Journal of Sound and Vibration*, 278(3), pp. 589–610

[16] Wang M. L., Xu F. L., Lloyd G. M. (2000) A Systematic Numerical Analysis of the Damage Index Method Used for Bridge Diagnostics, *Smart Structures and Materials 2000: Smart Systems for Bridges, Structures, and Highways*, Proceedings of SPIE, vol. 3, 988, Newport Beach, California, pp. 154–164

[17] Maeck J., De Roeck G. (1999) Dynamic Bending and Torsion Stiffness Derivation from Modal Curvatures and Torsion Rates, *Journal of Sound and Vibration*, vol. 225(1), pp. 153–170

[18] Akgun M. A., Garcelon J. H., Haftka R. T. (2001) Fast Exact Linear and Non-linear Structural Reanalysis and the Sherman-Morrison-Woodbury Formulas, *International Journal for Numerical Methods in Engineering*, 50, pp. 1587–1606

[19] Holnicki-Szulc J., Kolakowski P., Nasher N. (2005) Leakage Detection in Water Networks, *Journal of Intelligent Material Systems and Structures*, vol. 16(3), pp. 207–219

[20] Holnicki-Szulc J., Gierlinski J. T. (1995) *Structural Analysis, Design and Control by the Virtual Distortion Method*, J. Wiley & Sons, Chichester, U.K.

[21] Kolakowski P., Zielinski T. G., Holnicki-Szulc J. (2004) Damage Identification by the Dynamic Virtual Distortion Method, *Journal of Intelligent Material Systems and Structures*, vol. 15(6), pp. 479–493

[22] Kolakowski P. (2004) Damage Identification by the Static Virtual Distortion Method, *Engineering Transactions*, vol. 52(4), IFTR, Warsaw, pp. 253–270

[23] Mujica L. E., Vehi J., Rodellar J., Garcia O., Kolakowski P. (2004) Hybrid Knowledge Based Reasoning Approach for Structural Assessment, P*roc. of the 2nd European Workshop on Structural Health Monitoring*, 7–9 July, Munich, Germany, pp. 591–598

[24] Huo Z., Noori M., Amand R. S. (2000) Wavelet-based approach for structural damage detection, *Journal of Engineering Mechanics*, 126(7), pp. 677–683

[25] Hou Z. and Hera A. (2001) A system identification technique using pseudo-wavelets. *Journal of Intelligent Material Systems and Structures*, 12(10), pp. 681–687

[26] Chang C. C., Chang T. Y. P., Xu Y. G., Wang M. L. (2000) Structural damage detection using an iterative neural network, *Journal of Intelligent Material Systems and Structures*, 11(1), pp. 32–42

[27] Yana Y. J., Yam L. H., Jiang J. S. (2003) Vibration-based damage detection for composite structures using wavelet transform and neural network, *Composite Structures*, 60(4), pp. 403–412

[28] Chou J-H. and Ghaboussi J. (2001) Genetic algorithm in structural damage detection, *Computers & Structures*, 79(14), pp. 1335–1353

[29] Farrar C. R., Duffey T. A., Doebling S. W., Nix D. A. (1999) A statistical pattern recognition paradigm for vibration based structural health monitoring, *Structural Health Monitoring*, pp. 764–773

[30] Monaco E., Franco F., Lecce L. (2000) Experimental and numerical activities on damage detection using magnetostrictive actuators and statistical analysis, *Journal of Intelligent Material Systems and Structures*, 11(7), pp. 567–578

[31] Sohn H., Worden K., Farrar C. R. (2002) Statistical damage classification under changing environmental and operational conditions, *Journal of Intelligent Material Systems and Structures*, 13(9), pp. 561–574

[32] Natke H. G., Yao J. T. P. (1993) Detection and location of damage causing non-linear system behaviour, In: H. G. Natke, G. R. Tomlinson, and J. T. P. Yao, editors, Proc. of the International Workshop on "Safety Evaluation Based on Identification Approaches Related to Time Variant and Nonlinear Structures", Lambrecht, Vieweg, Braunschweig

[33] Kumar H. S., Krishnamoorthy C. S. (1996) Case-based reasoning in bridge design, In: *Advances in Computational Structures Technology*, pp. 197–205, Third International Conference in Computational Structures Technology, Budapest, Hungary, Civil-Comp Press

[34] Raphael B. and Smith I. (1998) Finding the right model for bridge diagnosis, In: Ian Smith, editor, *AI in Structural Engineering*, number 1454, Lecture Notes in Computer Science, pp. 308–319, Springer

[35] Kohonen T. (1990) The self-organizing map, *Proceeding in IEEE*, 78(9), pp. 1464–1480

[36] Chui C. K. (1997) *Wavelets: A Mathematical Tool for Signal Analysis*, SIAM, Philadelphia

[37] Mallat S. (1999) *A Wavelet Tour of Signal Processing*, 2nd ed., Academic Press

[38] Leake D. B. (1996) *Case-Based Reasoning: Experiences, Lessons, and Future Directions*, AAAI Press

[39] Pittner S. and Kamarthi S. V. (1999) Feature extraction from wavelet coefficients for pattern recognition tasks, *Pattern Analysis and Machine Intelligence, IEEE Transactions,* 21(1), pp. 83–88

[40] Kolakowski P. (2004) Damage Identification in Beams by Piezodiagnostics, P*roc. of the 2nd European Workshop on Structural Health Monitoring*, 7–9 July, Munich, Germany, pp. 775–782

[41] Friswell M. I., Mottershead J. E. (2001) Inverse Methods in Structural Health Monitoring, *Damage Assessment of Structures*, Proceedings of the International Conference on Damage Assessment of Structures (DAMAS'01), 25–28 June, Cardiff, UK, pp. 201–210